Research Article

Received: 11 March 2010 Revised: 30 June 2010 Accepted: 7 July 2010 Published online in Wiley Online Library: 24 December 2010

(wileyonlinelibrary.com) DOI 10.1002/pi.3004

Polyaniline-modified cellulose nanofibrils as reinforcement of a smart polyurethane

María L Auad,[a] Tara Richardson,[a] William J Orts,[b] Eliton S Medeiros,[b,c] Luiz HC Mattoso,[d] Mirna A Mosiewicki,[a,e] Norma E Marcovich[e] and Mirta I Aranguren[e]*

Abstract

Segmented polyurethanes exhibiting shape memory properties were modified by the addition of polyaniline (PANI)-coated cellulose nanofibrils (CNFs). The two-phase structure of the polymer is responsible for the material's ability to 'remember' and autonomously recover its original shape after being deformed in response to an external thermal stimulus. PANI was grown on the surface of the CNFs via *in situ* polymerization. Modified nanocrystals were added to the segmented polyurethane in concentrations ranging from 0 to 15 wt%. The changes in the material properties associated with the percolation of the coated fibrils appear at higher concentrations than previously observed for non-modified CNFs, which suggests that fibril agglomeration is occurring due to the PANI coating. The shape memory behavior of the composites is maintained at about the same level as that of the unfilled polyurethane only up to 4 wt% of fibrils. At higher concentrations, the rigidity of the nanofibrils as well as their interaction with the hard-segment phase and the increasing difficulty of dispersing them in the polymer collaborate to produce early breakage of the specimens when stretched at temperatures above the melting point of the soft segments.

Keywords: smart materials; nanocomposites; cellulose; polyaniline; shape memory

INTRODUCTION

Thermoplastic segmented polyurethanes (PUs) are materials that can be easily processed, showing high stretching capability and good solvent resistance. The chemistry behind their synthesis leads to a biphasic morphology consisting of hard segments (HSs) and soft segments (SSs). Depending on their morphology, PUs can show pseudo-elasticity or large recoverable strain, high damping capability and shape memory behavior, which is derived from the reversible phase transitions that these materials can undergo.[1]

Usually, the SSs are composed of polyols with typical number-average molecular weight of 500 to 2000 g mol^{-1} or higher, whereas the HSs are built from diisocyanates and short chain extenders.[2] HS interactions result in crystalline or glassy regions (in some cases, a chemically crosslinked polymer is utilized), which are responsible for the permanent shape of the material. However, these smart materials can have both a permanent stored shape and a temporary shape.[3] A reversible thermal transition of the SSs allows the fixing of a transient shape. The permanent form is 'remembered' by the 'frozen' phase, formed by the HSs. This phase is responsible for the shape recoverability of the polymer.

In the present study, the melting of the partially crystalline SSs is the thermal transition that allows the fixing of a transient shape. By heating the segmented PU up to a temperature T_s, which is higher than the phase transition temperature of the reversible phase (SS), its modulus drops and the PU becomes a soft extensible elastomer.[4] At this stage the polymer can be deformed and given a transient shape, which is fixed by lowering the temperature below the transition temperature. By re-heating the material above T_s, it recovers the original shape, which was stored by the 'undeformed' HS.

In a previous publication[5] it was shown that the addition of cellulose nanocrystals, which strongly interact with the PU, can: (i) change the temperature of the transitions by changing the molecules mobility; (ii) change the crystal structures by affecting the phase separation of PU segments; (iii) modify the relaxation processes of the polymer phases; and (iv) modify the mechanical/shape memory properties of the nanocomposites.

Cellulose was selected because is an abundant naturally occurring and renewable polymer, which can be used to obtain nanocrystals and nanofibrils. It also has hydroxyl groups that can

* *Correspondence to: Mirta I Aranguren, Institute of Materials Science and Technology (INTEMA), University of Mar del Plata, Mar del Plata 7600, Argentina. E-mail: marangur@fi.mdp.edu.ar*

a *Polymer and Fiber Engineering Department, Auburn University, Auburn, AL 36849, USA*

b *Western Regional Research Center, Agricultural Research Service, US Department of Agriculture, Albany, CA 94710, USA*

c *Department of Materials Engineering, Universidade Federal da Paraíba, João Pessoa – PB, 58051-900, Brazil*

d *Laboratorio Nacional de Nanotecnologia para o Agronegocio – LNNA, Embrapa Instrumentação Agropecuaria, São Carlos, 13560-970, SP, Brazil*

e *Institute of Materials Science and Technology (INTEMA), University of Mar del Plata, Mar del Plata 7600, Argentina*

strongly interact with other polar materials, such as PUs. This is important for obtaining a good dispersion of the cellulose in the polymer[6] and for obtaining good interfacial adhesion, which is essential for the fabrication of composites with good mechanical properties.

Additionally, polyaniline (PANI) was grown on the surface of cellulose nanofibrils (CNFs) using a technique that has recently been described by Mattoso *et al*.[7] Use of a conductive coating on the CNF surface could prove advantageous through the material exhibiting a response to electrical fields or showing electrostatic properties. The present paper reports an initial investigation of this type of material, where the main goal was to maintain the thermal shape memory response of the original polymer, while increasing its modulus through addition of CNFs, and to investigate possible changes in the electrical properties of composite films with addition of PANI-coated CNFs (PANI-CNF).

EXPERIMENTAL

Materials and preparation

A high-performance thermoplastic polyester PU (IROGRAN PS455-203, Hunstman) that exhibits shape memory behavior was selected as the matrix.

Cellulose crystals were prepared from microcrystalline cellulose (Avicel PH101 MCC, FMC BioPolymer, USA) by acid hydrolysis in aqueous suspension,[6] as follows. Microcrystalline cellulose was immersed in a sulfuric acid solution (64% w/v) in a ratio of microcrystalline cellulose to acid solution of 1 : 8.75 g mL^{-1}. The suspension was strongly stirred at 45 °C for 2 h. An equal volume of water was added to the suspension for washing, and this operation was repeatedly performed, each time separating the crystals from the liquid by centrifugation (12 000 rpm, 10 min) until reaching pH = 5. The final dispersion of the crystals in water was further improved by using a 10 min ultrasonic treatment (Ultrasonik 250, NEY).

Conductive cellulose crystals were prepared by *in situ* polymerization of PANI onto the nanocrystal surfaces. Aniline was dissolved (0.15% v/v) in an aqueous solution of HCl (1.0 mol L^{-1}). Then, 67 mL of the aniline solution was gently added to 50 mL of the CNF suspension (1% w/v). Finally, 50 mL of a solution of ammonium persulfate (APS) in aqueous HCl (0.25 g of APS in 50 mL of 1.0 mol L^{-1} HCl solution) was added in order to initiate the polymerization. The reaction was monitored by open circuit potential (V_{oc}) using platinum and saturated calomel electrodes. In the final stage, the end of the polymerization could be detected by V_{oc} measurements and visually when the color of the solution turned dark green, characteristic of the emeraldine oxidation state of conductive PANI. The resulting coated cellulose was washed repeatedly and finally dialyzed to obtain PANI-CNF dispersions.[7]

The PANI-CNF thus obtained were freeze-dried (Labconco Freeze Dryer 8) and then re-dispersed in dimethylformamide (DMF) using ultrasonication. Finally, this suspension was mixed with a DMF solution of the commercial PU in the proportions required to reach the PANI-CNF concentrations specified for the final materials. Composite films were prepared by casting and further solvent evaporation at 80 °C in a convection oven.

Characterization

CNFs (with and without PANI) as well as the surfaces of the cryo-fractured films were coated with gold and analyzed using SEM (Philips model SEM 505).

The CNFs were also characterized using Fourier transform infrared (FTIR) spectroscopy in attenuated total reflection mode. Spectra were recorded at 2 cm^{-1} resolution using a Genesis II FTIR spectrometer. Reported results are the averages of 32 scans.

The thermal degradation of the fibrils was investigated using thermogravimetry with a Shimadzu TGA-50 thermogravimetric analyzer at a heating rate of 10 °C min^{-1} under nitrogen atmosphere.

Composite samples in the molten state (at 160 °C) were subjected to rheological oscillatory testing in the linear viscoelastic range (small strains) with a model AR-G2 (TA Instruments) rheometer using parallel-plate geometry (diameter of 25 mm).

Modulated DSC (MDSC) testing of the samples was performed using a calorimeter (TA Instruments DSC Q2000) equipped with a cooling unit. Measurements were performed at 10 °C min^{-1} under nitrogen atmosphere (50 mL min^{-1}). The modulated temperature change was programmed with a sinusoidal oscillation of ±1 °C every 60 s.

Tensile tests were performed on rectangular specimens of 5 mm × 45 mm cut from the films. The tests were performed using an Instron 4400R (model 1122) universal testing machine at room temperature and 10 mm min^{-1} up to an elongation of 100%, and then the speed was increased to 100 mm min^{-1} to record the elongation at break.

The electrical conductivity of composites prepared with various concentrations of nanocrystals was determined at room temperature using *ad hoc* equipment (two-probe method). Samples were stored in desiccators above P_2O_5 for 3 days before testing, in order to eliminate absorbed moisture.

Shape memory behavior was tested by performing thermomechanical tensile cyclic tests on 5 mm × 25 mm film specimens using a universal testing machine equipped with a heating chamber (Instron 8501). The specimens were conditioned at 60 °C in the chamber and then elongated to 100% strain at a speed of 20 mm min^{-1}. The specimens were then rapidly cooled below room temperature and unloaded. In the final step of the cycle, the samples were heated once again to 60 °C and allowed to recover for 5 min. The thermomechanical cycle was repeated to complete four cycles.

The capabilities of maintaining the imposed transient strain and of recovering the original shape were determined as the 'fixity' and 'recovery' ratios (R_f and R_r, respectively), which were calculated from these tests as follows:[5,8]

$$R_f = \frac{\varepsilon_u}{\varepsilon_m} \times 100\% \quad (1)$$

$$R_r(N) = \frac{\varepsilon_m - \varepsilon_p(N)}{\varepsilon_m} \times 100\% \quad (2)$$

where ε_m is the maximum strain in the cycle, ε_u is the strain maintained after unloading and ε_p is the residual strain after re-heating and recovery. In this study, ε_m was fixed at 100%.

RESULTS AND DISCUSSION

Characterization of PANI-CNF

Figure 1 shows characteristic SEM images of the cellulose nanocrystals before and after PANI was grown on their surfaces. From the SEM analysis of the CNFs (Fig. 1(a)), the average diameter is determined as 30–45 nm, which indicates that the nanofibrils are formed by association of more than one cellulose crystal (diameters ≈ 5–10 nm).[9] Their length is of the order of micrometers, so that

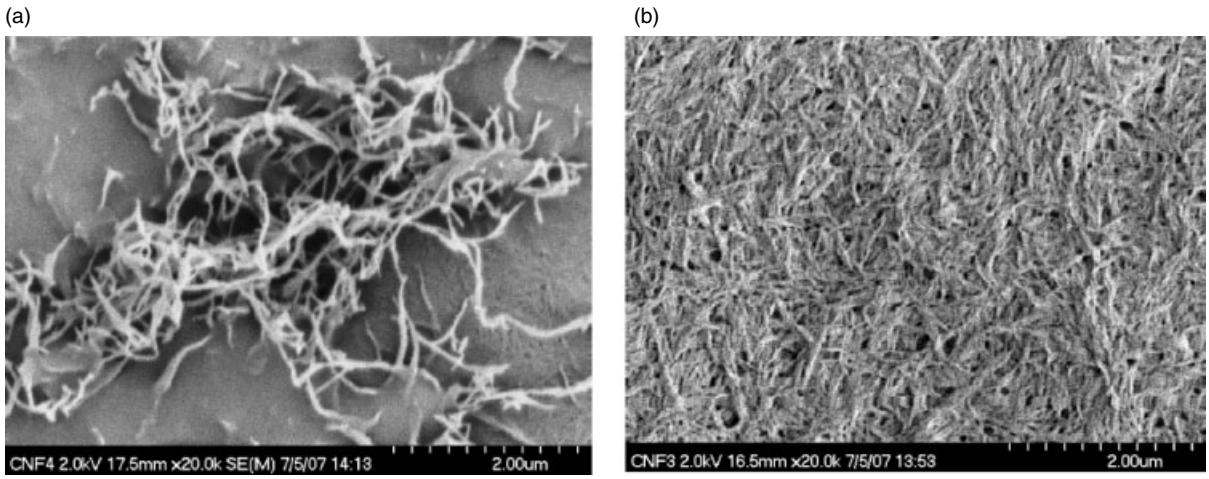

Figure 1. SEM images of (a) CNF and (b) PANI-CNF.

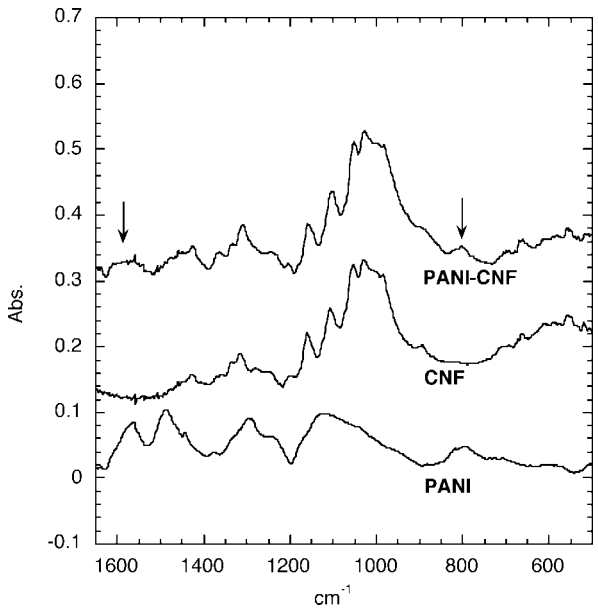

Figure 2. FTIR spectra of cellulose nanocrystals before and after *in situ* polymerization of PANI onto their surfaces. The spectrum of pure PANI is included for comparison.

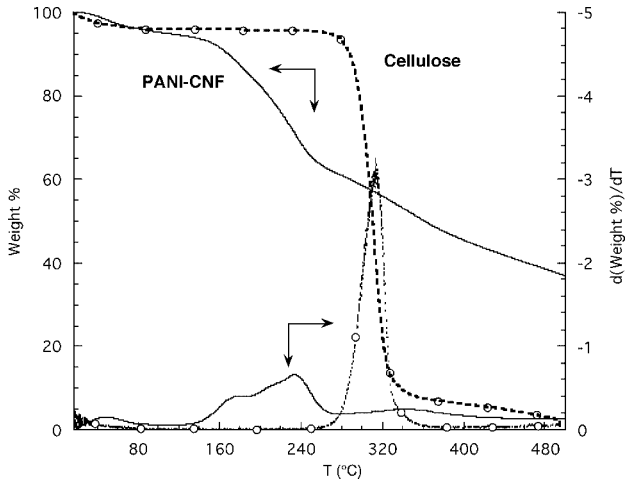

Figure 3. Results of thermal degradation of pure cellulose (Avicel PH101 MCC) and PANI-CNF. The weight of the samples (as % of the initial weight) and derivative signals are included.

the fibrils have a large aspect ratio. Figure 1(b) shows nanofibrils with PANI grown on their surfaces that were freeze-dried from aqueous suspension. Although the individual diameter of the fibrils does not appear to have changed much (which indicates a good distribution of the coating on the fibrils, as already previously discussed[7]), there is a certain degree of agglomeration. This effect is partially the result of drying during the preparation for the microscopy analysis, but could also be the result of the PANI brushes interlinking the fibrils. This feature has an important effect on the final properties of the nanocomposite films.

Comparison of the FTIR spectra (Fig. 2) of the CNFs before and after PANI growth shows a new peak at 806 cm^{-1} in the spectrum of PANI-CNF, which corresponds to the out-of-plane bending vibration of the C–H bonds of the benzene rings of PANI. There is also a small new band at 1570 cm^{-1}, which is assigned to the stretching vibration of the –N– in the quinoid moieties in the PANI chains in the doped form.[10]

Figure 3 shows the thermal degradation curve of PANI-CNF, together with that corresponding to unmodified cellulose. Analysis of the different responses illustrates the effect of PANI growth on the thermal degradation behavior of cellulose. The weight loss curve of neat microcrystalline cellulose shows just one peak corresponding to the thermal degradation of cellulose. The maximum degradation rate occurs at 313 °C and is very rapid, leaving essentially no residue (2.2 wt% in the present case). In contrast, the curve corresponding to PANI-CNF shows multiple steps of degradation. The initial weight loss that occurs below 100 °C corresponds to the removal of water, and possibly some HCl, from the sample. The thermal degradation appears as overlapping events that cover the range between 125 and 280 °C, followed by a degradation occurring at a lower rate above that temperature.

Clearly, the degradation begins at lower temperature for PANI-CNF than for pure cellulose, which is the result of the initial acidic hydrolysis of the fibrils and the acid medium in which the PANI growth takes place. However, of note is the much slower degradation rate of PANI-CNF, as well as the comparatively large residue left (36.98 wt% at 500 °C).

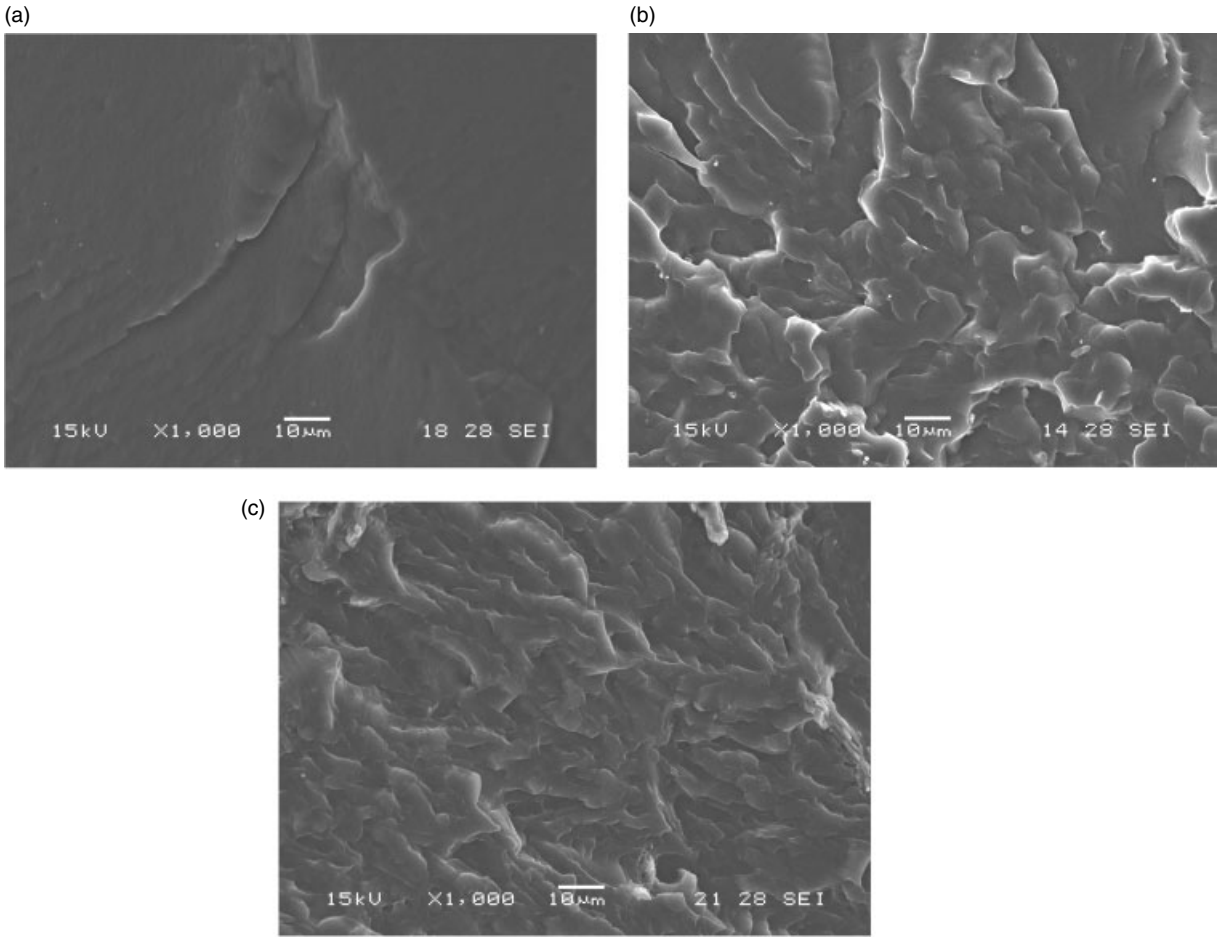

Figure 4. SEM images of cryo-fractured surfaces of PU with PANI-CNF at concentrations of (a) 0 wt%, (b) 4 wt% and (c) 10 wt%.

This interesting behavior was also observed by Stejskal *et al.*[10] for PANI-coated papers. Although the unmodified cellulose paper left essentially no residue, the coated paper left a 16–24 wt% char, a considerably higher percentage than the amount of PANI coating on the paper (less than 8 wt%). The authors reported that the cellulose was partially converted into carbon instead of forming gaseous components. It was also suggested that the pyrolitic residues of PANI deposited onto the cellulose act as a protective barrier, and thus cellulose partially converts to char, reducing the thermal degradation rate. The protective effect of PANI on the degradation of cellulose fibers has also been discussed by Mo *et al.*[11]

Characterization of nanocomposite films

SEM analysis

Figure 4 shows SEM images of the cryo-fractured surfaces of PU composite films containing various concentrations of PANI-CNF. The unfilled PU (Fig. 4(a)) shows an almost featureless surface, as expected for a neat polymer fractured under liquid air. Figure 4(b) shows increased roughness in the fracture surface of the sample with 4 wt% fibrils as compared with that of the unfilled PU, which is an obvious result of crack propagation stopped at points where the rigid cellulose particles deflect the crack towards an easier-to-fracture path. Figure 4(c), corresponding to the surface of the sample containing 10 wt% of PANI-CNF, shows also a very rough surface where the cracking path appears to be deflected with higher frequency, in correlation with the increasing concentration of fibrils. However, there are also some regions where aggregation of the fibrils appears (Fig. 4(c)). Inadequate dispersion is an almost inevitable problem at concentrations above the percolation threshold, such as in this case. Incorporation of relatively high amounts of nanofibrils leads to an increasing difficulty in dispersion and to some particle aggregation in the final material, which affect nanocomposite performance and will be further discussed.

Thermal characterization

The effect of the addition of modified cellulose nanofibrils on the thermal behavior of the segmented PUs was studied using MDSC. The first temperature scans were analyzed (after preparation and storage of the films for a week at room temperature).

The MDSC curves of the neat PU and composite films demonstrate the complexity of the system, showing various thermal events. Figure 5 shows the reversible, non-reversible and total heat flow traces corresponding to the neat PU, but these curves are also representative of the behavior of all composite samples. The reversible and total heat flow curves of Fig. 5 show more than one endothermic peak at high temperatures, which is probably the result of incomplete phase separation and formation of domains with different degrees of order. In spite of this, the most important features correspond to the melting of the SS and HS. The non-reversible flow curve clearly indicates that cold

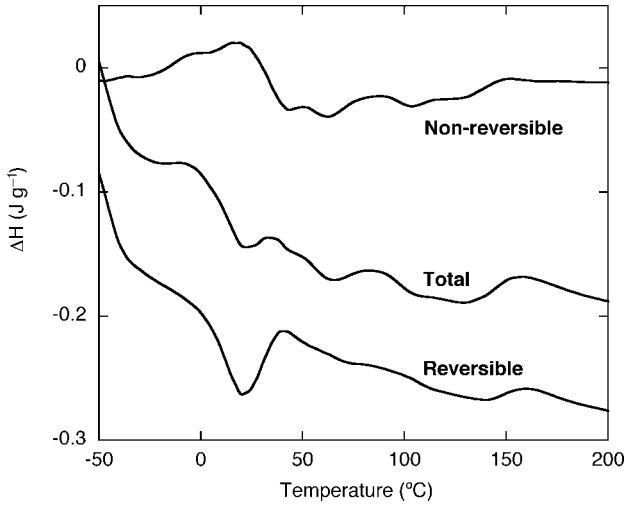

Figure 5. MDSC curves of neat PU film.

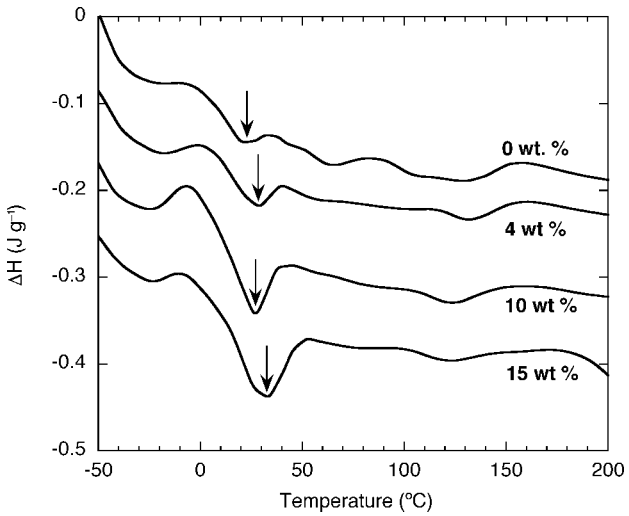

Figure 6. MDSC curves of composite PU films containing various concentrations of PANI-CNF.

crystallization and crystal perfection are also occurring almost during the whole heating step. For comparison, Fig. 6 shows the thermal behavior (total heat flow curves) of samples with various PANI-CNF concentrations. These results are also useful in illustrating the existence of a broad window interval between the melting temperatures of the two main domains, which is a necessary characteristic for the appearance of the shape memory behavior that is discussed further in a later section.

The thermal results obtained from the reversible MDSC traces are summarized in Table 1 and show that the overall trend is the increase of the melting point of the SSs with increasing PANI-CNF concentration. A similar trend is observed for the enthalpy of melting of the soft phase, which is about three times larger for the 15 wt% composite than for neat PU. These changes indicate that PANI-CNFs act to favor phase separation, leading to the formation of more perfect crystals and to a higher crystallinity (higher melting temperature and higher heat of melting, respectively). The effect of nanofillers as crystallization nucleating agents has been discussed in the literature in the case of silica-reinforced PU, where the crystallization of the SS phase also seemed to be preferentially

Table 1. MDSC characterization of neat PU and PANI-CNF composites (values obtained from the reversible heat flow traces)

PANI-CNF (wt%)	$T_{m,SS}$ (°C)	$T_{m,HS}$ (°C)	ΔH_{SS} (J g^{-1})	ΔH_{HS} (J g^{-1})	$\Delta H_{SS}/\Delta H_{SS,0\%}$
0	20.0	137.8	11.95	1.58[a]	1
4	27.8	145.6	10.67	0.27	0.89
10	26.7	132.2	25.39	0.37	2.12
15	32.2	133.3	31.47	0.32	2.63

[a] Corresponds to double peak area evaluated from 95 to 160 °C.

affected by the presence of nanoparticles.[12] Furthermore, this behavior was reported previously for a PU system containing unmodified cellulose nanocrystals[5] and was explained as the result of CNFs acting as heterogeneous nucleating agents for the polymer crystallization of the SSs. In that work, the enthalpy of melting associated with the SS phase content exhibited an increase of 80% with the addition of just 1 wt% of plain cellulose nanocrystals. Compared to those results, it appears that a higher PANI-CNF content is needed to obtain the same level of increase in the enthalpy of melting (between 4 and 10 wt%). It is interesting to note that the percolation threshold for unmodified CNFs was around 1 wt% and it is between 4 and 10 wt% in the PANI-CNF reinforced films, as will be discussed further in following sections.

Addition of 4 wt% of CNFs contributes to a better phase separation, as already discussed, and this is probably the reason for the HS showing a single melting peak slightly shifted towards higher temperatures. However, further addition of PANI-CNF seems to have a negative effect on the crystallization of the HSs, which melt at a lower temperature. This may be attributed, among other factors, to the nanofibrils interfering with the HS through hydrogen bonding, as well as to the PANI aromatic chains extending through the interface to form a 'blended interface' with the PU HSs. As a result, there is a reduction of the order needed for nucleation and growth and therefore a reduction in the crystallization of the HS phase.

Rheological characterization

At temperatures above the melting of the soft and hard phases, PU films (like any other molten thermoplastic) behave as viscoelastic liquids. The rheology of the filled melts was studied to investigate if the structure of the nanofibrils in the composites corresponds to separated fibrils/aggregates or to a spanning three-dimensional network.

Figure 7 shows the complex viscosity (η^*) *versus* frequency (ω) in the linear viscoelastic range (small strains) for composite PU films in the molten state at 160 °C. Clearly, the viscosity of the liquid increases with the PANI-CNF concentration, with the largest variations observed at low frequencies, where CNF structure is more effective in increasing the relaxation times of the material. The unfilled PU shows a Newtonian behavior with an essentially constant viscosity observed in the whole range of frequencies. However, addition of a low concentration of PANI-CNF produces a non-Newtonian response, and thus the viscosity is a function of the frequency for all the composites at concentrations above 4 wt%. Clearly, the curves obtained for the samples of higher concentration do not show a Newtonian plateau at low frequencies. Moreover, the viscosity curve of the 10 wt% sample shows a steep slope at low frequencies and the behavior of the 15

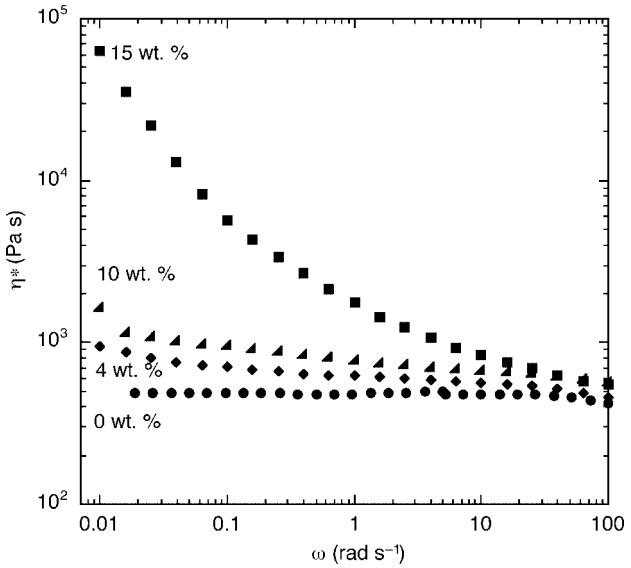

Figure 7. Complex viscosity of the melted PU composites containing various concentrations of PANI-CNF.

Table 2. Tensile properties of PU composite films containing various PANI-CNF concentrations

PANI-CNF (wt%)	Modulus (MPa)	Yield stress (MPa)	Elongation at break (%)
0	8.70 ± 1.43	1.51 ± 0.15	1664 ± 49
2	11.40 ± 1.76	2.17 ± 0.19	1537 ± 92
4	17.61 ± 2.07	2.81 ± 0.04	1112 ± 110
10	31.01 ± 2.35	3.15 ± 0.07	753 ± 22

wt% sample corresponds to that of a viscoelastic gel with viscosity increasing continuously (unbounded) as frequency decreases.

From these results, it is suggested that a qualitative change occurs in the range between 4 and 10 wt% of PANI-CNF, as was proposed in a previous section. The concentration threshold is much lower than usually found in macroscopic filler composites;[13] however, it is higher than that found previously for an unmodified CNF–PU composite.[6] The reason for this difference can be traced to the 'gluing' action of the PANI as it grows on the surface of the nanofibrils. The conductive polymer can act to link the nanofibrils, which consequently behave as thicker fibers of lower aspect ratio than their unmodified counterparts.

Mechanical properties

The films were tested under uniaxial extension and the results for their mechanical properties are reported in Table 2. The results for the unfilled thermoplastic PU are typical of an elastomer: rubbery modulus and high elongation at break. As expected, addition of PANI-CNF has the overall effect of increasing the elastic modulus of the films. There is no real yield stress in the response of the films. The value reported corresponds to the intersection of the extrapolated straight lines that can be drawn at small and large deformations. The values follow the same trend observed for Young's modulus, while the elongation at break is reduced. These results are expected for the reinforcement of an elastomer with rigid particles. However, the effect on the modulus is large at the concentrations used; for example, the corresponding value of the 10 wt% PANI-CNF sample is more than three times that of the unfilled PU. On the other hand, although the ultimate elongation is reduced, it is clear that the material can reach more than eight times its initial length before rupture, which is still a large extensibility.

Table 3. Electrical resistivity values of PU composite films containing various PANI-CNF concentrations

PANI-CNF (wt%)	Resistivity (Ω cm)
0	$>10^{11}$
2	$>10^{11}$
4	$>10^{11}$
10	2.2×10^{10}
15	2.7×10^{10}
100	5.3×10^{5}

Electrical conductivity

The electrical resistivity of films containing various concentrations of modified CNFs is summarized in Table 3. At concentrations of PANI-CNF below 4 wt%, the material is non-conducting, but above this concentration samples show some electrical conductivity. Although the conductivity of the samples is low (high resistivity) as a consequence of partial dedoping due to solvent (DMF) basicity, the method allows one to determine the concentration range at which the percolation of the coated nanofibrils occurs. The electrical percolation threshold appears in the range 4–10 wt% of PANI-CNF, the same concentration range at which the change in the rheological behavior takes place. The low values obtained suggest that higher doping should be tried to obtain more interesting electrical properties.[9] The use of dopants other than HCl or increasing the HCl concentration before freeze-drying or even during nanocomposite preparation could be considered. The use of higher concentrations of coated CNFs could be another option, but that might lead to reduced extensibility and eventually to the loss of the shape memory properties. Similarly, thicker PANI coatings on the nanofibrils might result in more agglomeration of the fibrils.

Shape memory behavior

While the addition of PANI-CNF to the films improves Young's modulus, it is still necessary to verify that the original shape memory properties of the PU are not lost by such addition.

Figure 8 shows the curves representing the response of the commercial unfilled PU under thermomechanical cycling. The high temperature of the cycle was chosen as $T_s = 60\,^{\circ}C$, a temperature higher than the melting of the SSs and lower than the melting of the HSs. At this temperature, the tensile response of the material is that of a soft elastomer: the SS chains exhibit large mobility and the hard phase imposes restrictions by acting as 'physical crosslinking domains'. After elongation the material is frozen between the grips and the strained shape is fixed because of the reduced Brownian motion of the molecules. The sample is then allowed to relax between the grips, by reducing the load to zero. Next, the specimen is heated again at T_s, which results in a substantial recovery of the original shape when the chains recover the high-temperature mobility.

As reported by various authors, the first cycle is different from the subsequent ones[14–16] due to the rearrangement of the domain morphology that occurs during the first deformation at high temperature. However, the material response becomes

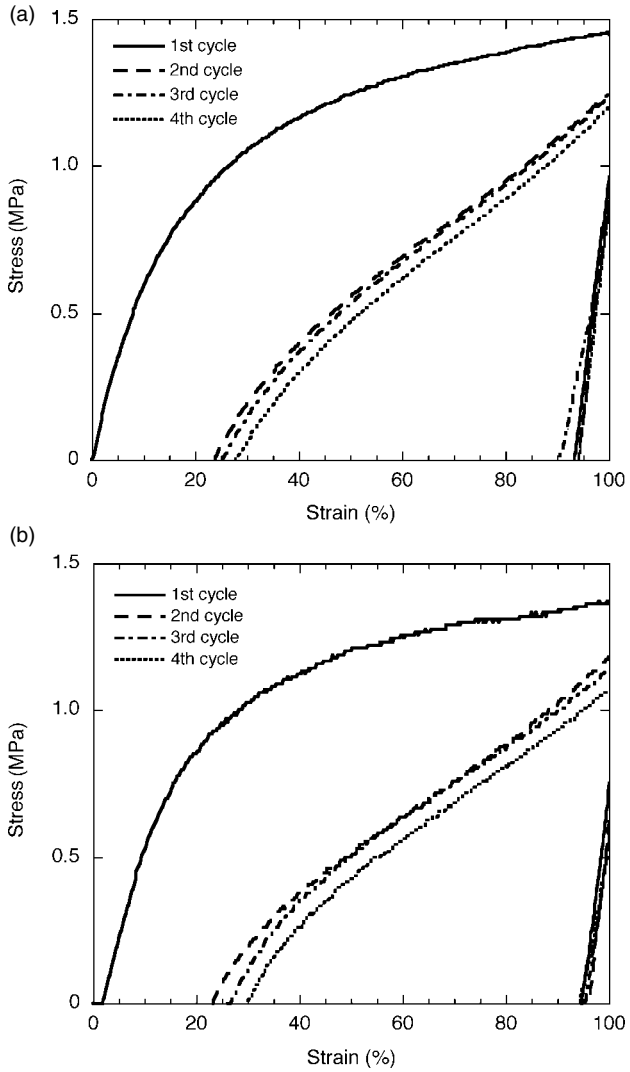

Figure 8. Plots of thermomechanical tensile response of (a) neat PU and (b) 2 wt% PANI-CNF composite.

repeatable with subsequent cycling. This feature is also observed for the composite films.

Table 4 summarizes the results for the unfilled sample and for two composite films of different PANI-CNF concentrations. While the addition of high concentrations of PANI-CNF increases the tensile modulus of the PU (as already discussed), it also leads to reduced elongations at break. The effect is important during the high-temperature step of the cycle during which the sample is elongated; for example, the 10 wt% composite breaks at about 35% elongation. It should also be noted that increasing PANI-CNF concentrations produces larger interactions with HS blocks, interfering in the arrangement of this phase.[5] Increasing dispersion problems should not be underestimated in this respect. The material may still be suitable for some applications, but it does not offer the advantage of large extensibility, which is one of the characteristics of PU intended to be preserved, while increasing the modulus.

The fixity and recovery of the samples were calculated according to Eqns (1) and (2). From the results, a recovery is observed between 63 and 78% for all samples up to the fourth cycle, at least. Although the recovery calculated with respect to the 100% elongation may seem low, the repeatability of the results in subsequent cycles should be considered. If the actual strain of the already tested samples (after the first cycle) is considered ($\varepsilon_m - \varepsilon_p$), the calculated recoveries would be higher than 85%.

The fixity is above 90%, with the exception of the third and fourth cycles of the 4 wt% sample. This drop in fixity of the 4 wt% sample as cycling progresses is suggested to be the result of the interactions of the PANI-CNF with the HS phase of the PU, which lead to increasing morphology disruption during cycling. However, further cycling proves to be repeatable at the elongation used in the study.

CONCLUSIONS

The results show that it is possible to use PANI-CNF as nanoreinforcement for segmented PU. The thermal, rheological and electrical measurements show a stepwise change in properties in the range 4–10 wt% nanofibrils, indicating that there is a transition in the responses of the composites, below and above percolation. However, to get more useful electrical properties, the PANI-CNF should be re-doped after being synthesized or during mixing with PU, since the basicity of the solvent used may have caused partial de-doping of PANI.

The shape memory behavior of the composites is maintained at about the same level as that of the unfilled PU only up to 4 wt% of fibrils. At higher concentrations of PANI-CNF, the rigidity of the nanofibrils as well as their interaction with the HS phase and the increasing difficulty of dispersing them in the polymer collaborate to produce early breakage during tensile tests at a temperature T_s, higher than the melting temperature of the SSs.

The use of conductive CNFs opens the future possibility of triggering the shape memory response of these cellulose–PU composites through the use of a stimulus other than temperature, although PANI deposition should be optimized for that purpose.

ACKNOWLEDGEMENTS

The authors acknowledge the financial support from CONICET, ANPCyT and UNMdP in Argentina. MIA also thanks the Guggenheim Foundation. MLA thanks the Department of Commerce, USA. Finally, thanks are also due to Huntsman Polyurethanes for

Table 4. Shape memory behavior (fixity and recovery percentages calculated from Eqns (1) and (2))

	First cycle		Second cycle		Third cycle		Fourth cycle	
PANI-CNF (wt%)	R_f (%)	$R_r(1)$ (%)	R_f (%)	$R_r(2)$ (%)	R_f (%)	$R_r(3)$ (%)	R_f (%)	$R_r(4)$ (%)
0	91.8 ± 1.7	76.8 ± 8.1	90.2 ± 2.8	72.5 ± 8.2	90.3 ± 0.4	64.1 ± 9.3	93.2 ± 0.8	62.6 ± 9.5
2	95.1 ± 0.5	77.0 ± 4.2	94.5 ± 2.1	73.9 ± 13.5	93.7 ± 2.4	69.4 ± 14.9	93.6 ± 0.8	64.6 ± 13.8
4	90.7 ± 2.8	75.0 ± 17.9	91.5 ± 4.5	73.6 ± 14.5	73.0 ± 0.7	71.2 ± 14.1	78.4 ± 9.0	65.1 ± 2.36

kindly supplying the shape memory PU; and to FINEP/LNNA and Embrapa/LABEX, Brazil.

REFERENCES

1 Wei ZG, Sandström R and Miyazaki S, *J Mater Sci* **33**:3743–3762 (1998).
2 Kim BK, Lee SY and Xu M, *Polymer* **37**:5781–5793 (1996).
3 Tobushi H, Hara H, Yamada E and Hayashi S, *Smart Mater Struct* **5**:483–491 (1996).
4 Jeong HM, Lee SY and Kim BK, *J Mater Sci* **35**:1579–1583 (2000).
5 Auad ML, Contos V, Nutt S, Aranguren M and Marcovich N, *Polym Int* **57**:651–659 (2008).
6 Marcovich NE, Bellesi NE, Auad ML, Nutt SR and Aranguren MI, *J Mater Res* **21**:870–881 (2006).
7 Mattoso LHC, Medeiros ES, Baker DA, Avloni J, Wood DF and Orts WJ, *J Nanosci Nanotechnol* **9**:2917–2922 (2009).
8 Behl M and Lendlein A, *Mater Today* **10**:20–28 (2007).
9 Eichhorn SJ, Dufresne A, Aranguren M, Marcovich N, Capadona JR, Rowan SJ, *et al*, *J Mater Sci* **45**:1–33 (2010).
10 Stejskal A, Trchova M and Sapurina I, *J Appl Polym Sci* **98**:2347–2354 (2005).
11 Mo ZL, Zhao ZL, Chen H, Niu GP and Shi HF, *Carbohydr Polym* **75**:660–664 (2009).
12 Nunes RCR, Pereira RA, Fonseca JLC and Pereira MR, *Polym Test* **20**:707–712 (2001).
13 Marcovich NE, Reboredo MM, Kenny JM and Aranguren MI, *Rheol Acta* **43**:293–303 (2004).
14 Koerner H, Price G, Pearce NA, Alexander M and Vaia RA, *Nature Mater* **3**:115–120 (2004).
15 Lin JR and Chen LW, *J Appl Polym Sci* **69**:1563–1574 (1998).
16 Gall K, Dunn ML, Liu Y, Finch D, Lake M and Munshi NA, *Acta Mater* **50**:5115–5126 (2002).

